Proceedings of IMECE2005
2005 ASME International Mechanical Engineering Congress and Exposition
November 5-11, 2005, Orlando, Florida USA

IMECE2005-81514

MODELING AND DESIGN OF HEAVY DUTY HYBRID ELECTRIC VEHICLES

Pierluigi Pisu
Center for Automotive Research
The Ohio State University
930 Kinnear Road
Columbus, Ohio 43212, USA
e-mail: pisu.1@osu.edu

C. Hubert, N. Dembski, G. Rizzoni
Center for Automotive Research
The Ohio State University
930 Kinnear Road
Columbus, Ohio 43212, USA
e-mail: hubert.11@osu.edu, dembski.5@osu.edu, rizzoni.1@osu.edu

John Josephson
Computer Science and Engineering Department
The Ohio State University
2015 Neil Ave.
Columbus, Ohio 43210, USA
email: jj@cis.ohio-state.edu

James Russell, Mark Carroll
Aetion Technologies LLC
1275 Kinnear Road
Columbus, Ohio 43212, USA
email: James.Russell@aetion.com, Mark.Carroll@aetion.com

KEYWORDS
Hybrid electric vehicle, modeling, design space exploration.

ABSTRACT
A large scale design space exploration provides invaluable insight into vehicle design tradeoffs. Performing such a search requires designers to:
- define appropriate performance criteria by which to judge the vehicles in the design space;
- develop vehicle models to calculate the needed criteria; and
- determine suitable velocity profiles as well as grade and terrain conditions to feed into the models.

This paper presents a methodology for creating and conducting a design space exploration with particular application to heavy duty series hybrid electric-trucks.

INTRODUCTION
Modern vehicle design is far from a simple single valued optimization process: truck and car manufacturers have a very wide number of evaluation criteria upon which their vehicles must be judged. Computers can be used in analytic or numeric optimization routines to provide the best configuration when evaluated on a single metric. However, when more than one criterion is used a "true" optimum generally does not exist. Typically different configurations maximize different criteria and one must make trade-offs amongst them. Many approaches look to use "weighting functions" to combine multiple criteria into a single criterion which can be optimized. In principle a weighting function should exist for the designers' or consumers' preferences. But in practice—particularly when there are many criteria—they are difficult if not impossible to analytically define. This work uses a different approach allowing the computer and the designer to interactively explore the tradeoffs after the computer has first eliminated all the clearly inferior candidates. Development and use of a tool for multi-criteria design space exploration can serve as a part of the vehicle design process, but it is does not represent the entire process. One must also decide what criteria to use in the evaluation and then perform the tests or simulation to obtain the criteria. This work looks to present an integrated process for vehicle design: developing drive/duty cycles used to test the vehicles, developing and using a simulator to model the vehicles as they are subjected to the duty cycles, and exploring the simulation results to identify good powertrain candidates.

Designing a hybrid electric—or any kind of—vehicle requires due consideration of the vehicle's intended use and the different driving conditions which the vehicle will undergo. Driving cycles provide information on opportunity for energy recuperation and power/energy requirements from the vehicle that allow a first cut sizing of its components [1]. Evaluation of vehicle candidates, particularly when based on fuel economy metrics, requires proper drive and duty cycles. Different candidates will be better suited to different cycles; worthwhile conclusions can only be drawn from evaluations based on appropriate drive and duty cycles [2]. A methodology developed to generate drive cycles based on a given mission profile and vehicle and soil characteristics is briefly described. Designing driving cycles (as well as modeling and designing vehicles) for off-road operation requires an appropriate model of the vehicle-soil interaction. This work uses the Bekker mobility model, developed by M.G. Bekker [3,4,5].

Vehicle modeling and simulation constitutes another of the key elements in the design space exploration process [6]. The

biggest challenge is to create the appropriate model for the intended use which contains a suitable level of detail to properly calculate the performance measures. This paper will present quasi-static series hybrid energy models and a backward simulator for heavy-duty trucks which function as key components of a design space exploration. The model is based on an improved version of the approach proposed by Rizzoni [7]. A vehicle model has three main blocks: a driving cycle block, a vehicle dynamics or load block, and a powertrain block. The driving cycle block supplies the inputs for the simulation, i.e. velocity profile, grade profile, and terrain information. The vehicle loads block uses these inputs to determine the actual forces and speeds which the powertrain must develop as well as the actual profile which the vehicle can meet. The powertrain block incorporates the latest technology among vehicle design options, including scalable ultracapacitor and NiMH battery packs as well as a variety of generator, engine and traction motor configurations.

Meaningful comparisons require appropriate drive cycles exist to properly test the vehicles. Further, meaningful comparisons require that the tests be properly run, evaluating each candidate when functioning properly. To test hybrid vehicles (be it through simulation, on the dyno or on the road), one must appropriately control the powertrains. A good powertrain design could still perform poorly under poor control, giving test results that do not really represent the true powertrain capabilities. Control strategies for hybrid-electric vehicles generally target several simultaneous objectives [8,9]. Here, different candidates will be compared based on fuel economy, so control efforts are focused on minimizing fuel consumption. Testing (done through simulation) then shows the true potential of the powertrain system and one can use the results to make definitive comparisons.

Regardless of the topology of the system, the essence of the HEV control problem is the instantaneous management of the power flows from the various energy storage devices (fuel tank, batteries or ultracapacitors) to achieve the overall control objectives. The proposed power split algorithm is based on an instantaneous Equivalent Consumption Minimization Strategy (ECMS) [10,11]. This approach is generic in nature, i.e. independent from the powertrain configuration (parallel, series, power split, etc.) and also independent from the particular powertrain components (engines or fuel cells, batteries or supercapacitors, etc.). The solution provided by the ECMS may not be optimal in a rigorous sense; however, the results presented by Pisu [12] show that the robustness, flexibility, and simplicity of the ECMS provide an intelligent and reliable way to perform design space exploration in a reasonable amount of time and with a reasonable computational effort.

After one has developed appropriate simulators and drive cycles, one can use them to evaluate vehicles. This work uses the evaluation tool as part of a large scale design space exploration. Another software package establishes a large design matrix with every possible design combination and runs multiple simulations on each candidate collecting several metrics from each test (simulation). After exhaustively simulating all candidates, the results are filtered [13] removing candidates that are clearly inferior without making any tradeoff decisions, leaving a Pareto optimal subset. Finally, the software lets the user interact with the remaining candidates, to explore the remaining trade-offs between different metrics (e.g. top speed and fuel economy). This approach to design space exploration [14] lets computers to do what they do well—looping through a large number of simulations, considering all possible combinations of different powertrain components and making simple decisions to eliminate clearly inferior candidates—while keeping the human "in the loop" to explore trade-offs and make final judgments [6].

DRIVING CYCLES

The authors have developed a methodology to generate drive cycles for heavy duty trucks. This methodology incorporates the particular mission profile of the specific vehicle platform and the expected limits of the vehicle's powertrain, but still allows existing driving cycles to be leveraged. Three basic steps form the core of the drive cycle generation: determination of the vehicle's mission profile; determination of the vehicle's maximum attainable speeds and accelerations over the specified terrains within the mission profile; and construction of cycles that match the mission profile but do not exceed the speed and acceleration limitations. Vehicle design specifications often include mission profiles (e.g. Table 1), which give details on the types of driving conditions the vehicles will see and the amounts of time for which it will see them. If specifications do not give mission profile information, completion of step 1 requires the designer to generate the mission profile given the vehicle's intended use.

The next step in the methodology is to determine the maximum attainable speeds and accelerations for each terrain condition in the mission profile. In order to do this, both a vehicle powertrain model and a vehicle-soil interaction model must be developed. The vehicle powertrain model is used to determine the power-limited maximum accelerations and speeds, and the vehicle-soil interaction model is used to determine the traction-limited maximum accelerations and speeds. The lower of the two values is the maximum attainable acceleration or speed for that specific terrain conditions. Using a vehicle powertrain model to help generate driving cycles can lead to a "chicken and egg" syndrome. Cycles are needed to test the powertrains, while powertrains are needed to develop the cycles. In truth, there is necessarily a relationship between the powertrains and the tests used to evaluate them; however this does not mean that the situation degrades to a vicious circle. Drive cycle development requires enough information to approximately characterize the expected tractive power and tractive force. At a minimum, one should know the desired maximum speed (giving an idea of peak power) and maximum gradeability (giving an idea of the peak force). In other situations, one may have an existing conventional powertrain from a similar vehicle which can serve as a baseline. When an existing powertrain exists, the model can take the power available at the engine and determine the maximum force available at the wheels under peak acceleration conditions for each transmission gear. An example of required component parameters for the model is presented in Table 2. The maximum attainable acceleration is then calculated from the maximum force available. When looking to match a given powertrain (as opposed to being given a desired top speed), top speed can be estimated given the peak power and efficiency characteristics along with the running resistance curve.

To calculate the maximum force available at the wheels, the maximum torque at the engine is multiplied by an

appropriate torque converter ratio (the full stall ratio is used in low gear, but in high gears little if any extra multiplication is available), the transmission gear ratio, the final gear ratio, and the powertrain efficiency. The losses across the powertrain are factored into the model through the multiplication of the powertrain efficiency. This gives the torque available at the wheels. Finally, this torque available at the wheels is then divided by the tire radius to give maximum force available at the wheels. Since there are seven transmission ratios for this vehicle, seven different force values are calculated.

The vehicle-soil interaction model used to determine the traction-limited maximum accelerations and speeds is based upon M.G. Bekker's mobility model [3,4,5]. The Bekker mobility model uses the relationship between certain physical soil characteristics and shearing strength to predict vehicle cross-country mobility. Bekker developed models for both wheeled and tracked vehicles, considering wheels and tracks to be simple loading surfaces having similar forms, but different lengths and widths. The fundamental basis of the Bekker model is equations of vehicle-soil interaction relating soil shear stress to the loading of the vehicle. These equations are empirical by nature and rely on seven unique soil parameters that are based on Bevameter measurement techniques for soil properties. Hence, the Bekker model is dependent on a large amount of field testing.

Table 1. Mission profile.

Pct of Cycle	Terrain Conditions
0.2	Hard Surfaced Roads – Dry Pavement
0.166	Secondary Roads – Dry Pavement/Gravel
0.166	Secondary Roads – Dry Packed Dirt
0.166	Secondary Roads - Mud
0.15	Level Cross Country
0.15	Hilly Cross Country

For the first two sections of the mission profile where the terrain is considered dry pavement and/or gravel, the traction-limited maximum force developed at the wheel was calculated using a standard coefficient of friction-limited normal force calculation. In both the cases, the coefficient of friction was assumed to be 0.8, and the normal force was calculated by multiplying this value by the vehicle weight. For the remaining sections of the mission profile, the Bekker model estimated the maximum thrust developed at the wheels as well as the rolling resistances seen due to the terrain. Having calculated the tractive force based on the limits of both the powertrain and the terrain-tire interface, one can compare the two and select the smaller value as the true "maximum" at the particular operating point.

The final step in the determination of the maximum attainable accelerations and speeds is the use of a simple vehicle dynamics road load model to determine acceleration and/or vehicle speed. The road load model includes the vehicle's rolling resistance, aerodynamic drag, and inertial properties. Finally, one can use the peak acceleration and velocity characteristics to develop the new cycle. Two types of cycles have been developed: synthetic, linear-modes cycles, and a cycles composed of existing real-world heavy-duty driving and grade data. Software has been developed to generate cycles which either run a desired amount of time or travel a desired distance. The mission profile is then used to determine the fraction of the cycle over which each terrain type is traveled. Each of these cycle segments is then developed separately from the other segments depending on the type of cycle desired. A flow chart summarizing the entire cycle development process is shown in Fig. 1.

Table 2. Powertrain model component parameters.

Engine	
Maximum Power [kW]	246
Maximum Torque [Nm]	1128
Inertia [kg-m^2]	3.74
Torque Converter	
Stall Ratio	2.20
Ratio at High Speed	0.80
Transmission	
1st Gear Ratio	6.93
2nd Gear Ratio	4.185
3rd Gear Ratio	2.2237
4th Gear Ratio	1.691
5th Gear Ratio	1.2
6th Gear Ratio	0.9
7th Gear Ratio	0.783
Final Gear	
Gear Ratio	7.8
Wheel	
Number of Tires	6
Tire Diameter [m]	1.18
Tread Height [m]	0.0238
Contact Patch Print Length [m]	0.325
Contact Patch Print Width [m]	0.297
Standard Inflation Pressure [kPa]	441
Other Parameters	
Powertrain Efficiency [%]	80.58

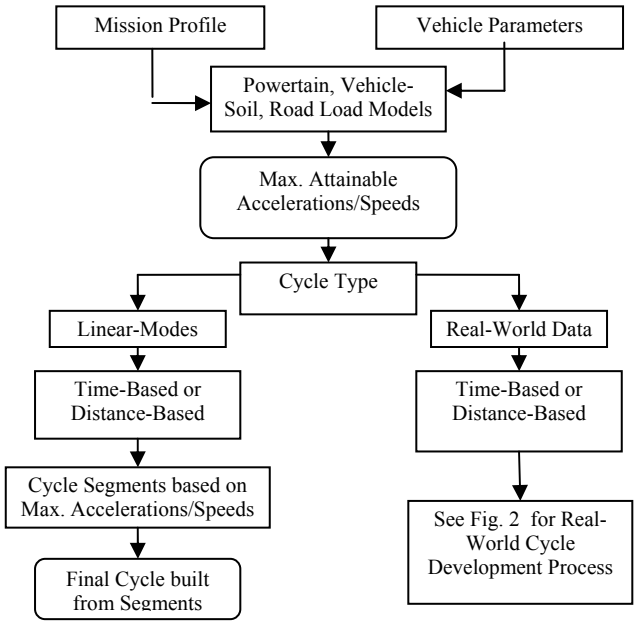

Fig. 1. Cycle development process.

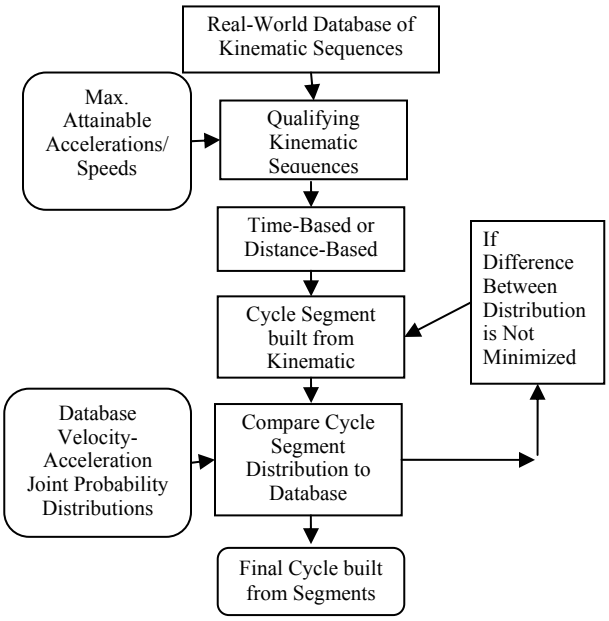

Fig. 2. Real-world cycle development process.

The linear cycle segments contain a five-second idle period followed by a period of linear acceleration at the maximum acceleration rate to the maximum speed. Then, a period of cruising at the maximum speed is followed by a period of linear deceleration at the maximum acceleration rate. The real-world data cycles requires a database from which to choose kinematic and grade sequences. A kinematic sequence contains a vehicle idle period followed by a period of vehicle movement. Real velocity traces (from actual vehicle measurements) provide the kinematic sequences. Grade profiles are collected with the velocity information. Each grade profile defines the grade which was present as the vehicle was being driven through the accompanying kinematic sequence. A flow chart summarizing the real-world cycle development process is shown in Fig. 2.

VEHICLE MODELING AND SIMULATOR

Overview of models and backward facing simulator

Two backward simulators have been created, one for the conventional vehicle and one for the hybrid electric vehicle. These simulators are quasi-static energy models of the vehicle, i.e. they capture only slow dynamics which are sufficient to analyze the system behavior from an energy point of view. Figure 3 represents the general simulator structure. At the top level, the following blocks form the basis of both the conventional and the series simulator.

- a driving cycle block;
- a vehicle dynamics or load block;
- a powertrain block;

The driving cycle block contains all the information for each driving cycle, i.e. velocity profile, grade profile, terrain information, and other information regarding auxiliary loads that are not currently used. The vehicle load block contains all the information related to the vehicle dynamics, e.g. mass, frontal area, drag, rolling resistance, Bekker model [3,4,5] for calculation of traction forces on different types of terrain, weight transfer, etc. While the series and conventional simulators use the same driving cycle and vehicle load blocks, simulation of the different powertrains naturally requires the use of different powertrain blocks.

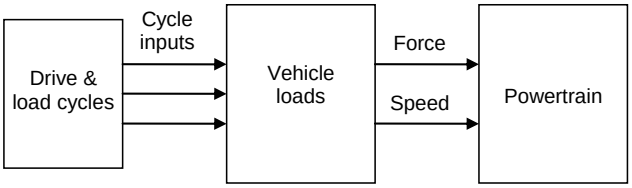

Fig. 3. Basic information flow in a backward simulator.

A conventional powertrain can be modeled by the following blocks: Wheel, Axle, Transmission, Clutch/ Torque converter, Engine Accessories, ICE (internal combustion engine), Fuel Tank, Radiator and Fan, Control unit (primarily determines gear ratio based on speed and needed power.)

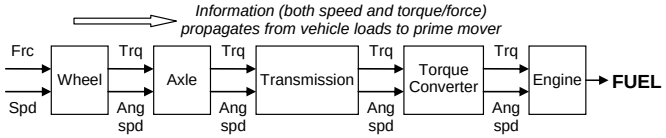

Fig. 4. Information flow within the powertrain block for a backward facing model of a conventional vehicle.

Figure 4 illustrates the basic information flow within the powertrain block of a backward facing model. To provide scalability, the ICE block uses maps and tables expressed in terms of mean piston speed and mean effective pressure (as defined in Heywood, [15]) as opposed to RPM and torque and mean available pressure as opposed to fuel consumption. (Mean available pressure represents the mean effective pressure which would result if all the energy in the fuel were converted to mechanical energy.) Users can then scale the original engine map up or down by entering a larger or smaller volumetric displacement—to quickly explore the impact of engine size on the design tradeoffs. The conventional model also allowed users to adjust the final drive ratio, by adjusting the gear ratio within the axle block.

The series hybrid powertrain model uses the following blocks: Wheel, three Axles, three Gearboxes, three Traction Motors, three Inverters/Rectifiers, RESS (rechargeable energy storage system, comprised of batteries or ultracapacitors), RESS electronics, Generator, ICE, Controller Unit with ECMS strategy, Various electrified accessories, Mechanical engine accessories (NB model looked at electrifying some accessories, others were modeled as engine driven) , Fuel Tank.

The ICE, axle and wheel blocks are identical to those in the conventional model. The RESS block contains information about several types of batteries and several types of supercapacitors. An input parameter allows any of the configurations to be selected for use in a given vehicle. Size of the RESS can be varied by selecting the number of storage units in series and the number of parallel branches. The controller unit implements the ECMS control strategy as will be described in the next section. The traction motor blocks contain a scalable map to determine the efficiency from the torque and speed. Scalability is made with respect to torque. The generator block contains a scalable map to calculate the efficiency and electrical power output to the electric bus. Note that electric machine (motor or generator) scaling is based on the actual practice of using a common stator/rotor laminate for

several sizes of electric machines. More powerful machines use longer stator/rotors (more laminates) and torque is seen to be nearly linear with length.

The preliminary study described here varied the generator and the engine sizing together. For each engine the generator was sized as one might size an industrial generator—with the continuous power rating of the generator approximately matching the engine power. More recent studies have looked at independently sizing the generator (relative to the engine), to determine what level of generator "overdesign" the series hybrid application really requires. Here "overdesign" refers to the amount by which the continuous rated power of the generator must exceed the average load it sees during an entire cycle. Proper functioning may require some degree of overdesign; while the generator can operate above its rated power it can only do so for a limited time. Extended periods of operation above the average power level, require overdesign to prevent overheating. However, the series hybrid application has different genset demands than a typical industrial installation. The generator will not always operate at or even near the peak engine power, thus a smaller generator may still provide proper durability and reliability.

Additional forward facing path

Addition of a "forward facing" simulation path allows the simulator to conduct acceleration tests (which simulate the vehicle at maximum power) and to indicate when a powertrain cannot meet a given driving schedule. Figure 5 shows a more detailed view of the information flow, adding the forward facing loop to the basic structure shown in Fig. 3. Again, the drive and load cycles block supplies information regarding the terrains, grades, and velocities. Initially, however, the vehicle loads block sends a desired speed to the powertrain block. The powertrain block then determines the maximum tractive force which can be produced at that speed and passes it back to the vehicle loads block. Using the maximum force (at the desired speed), the vehicle loads block can check to see if the desired trace can be met, and, if not, appropriately saturate the trace. In the event of an acceleration test, the vehicle loads block can use the maximum force to determine how much time the vehicle needs to accelerate to the given speed.

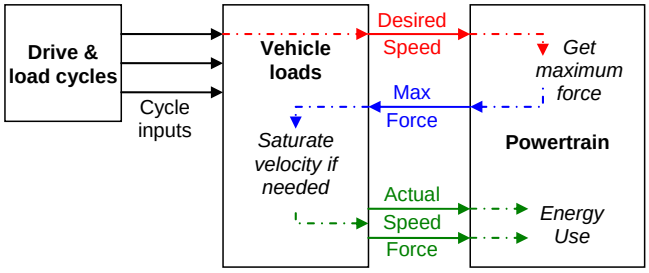

Fig. 5. Information flow in the backward simulator with additional forward facing path

Performance metrics

There are two basic types of test: "acceleration" tests, where the vehicle should go as fast as possible, and "driving cycles" where the vehicle should follow a pre-defined profile. The following list provides the performance metrics used for this study:

Acceleration outputs

- Top speed (in MPH)
- 0-50 MPH time
- 0-30 MPH time
- Distance traveled in 10 seconds
- Ability to move on terrain/grade (basically a flag—as long as top speed>0 this is 1)

Driving cycle outputs (Used for both conventional and series hybrid)

- Net fuel consumption (gallons)
- Gallons per hour ("raw"—ignoring any net changes in rechargeable energy)
- Cycle potential for recovery (percentage of energy to wheels which could potentially be recovered)
- Maximum velocity error
- RMS velocity error
- Percent distance "error" resulting from velocity error
- Increase in powertrain mass (Mass of current configuration minus that of the "stock" conventional vehicle. Can be negative if new powertrain is lighter than "stock" powertrain.)

Additional driving cycle outputs for series hybrids

- Net electricity used
- Equivalent gallons per hour (includes "equivalent" cost of electricity)
- Percent of "potentially recoverable" energy which was actually recovered and returned to bus
- Percent of allowable state of energy (SOE) range which was used during cycle
- Traction motor thermal stress factor (TMTSF). This is the ratio of the total heat losses which occur throughout the cycle (at actual motor torque and speed operation) to the heat losses which would occur if the motor were to operate at rated torque (at speeds determined from cycle) throughout the cycle. (Note that any loss is assumed to be dissipated as heat.)

$$TMTSF = \frac{\int_0^{T_f} \left[P_{elec}\left(T_{cyc}, \omega_{cyc}\right) - T_{cyc}\omega_{cyc}\right] dt}{\int_0^{T_f} \left[P_{elec}\left(T_{rate}\left(\omega_{cyc}\right), \omega_{cyc}\right) - T_{rate}\left(\omega_{cyc}\right)\omega_{cyc}\right] dt}$$

- Traction motor percentage of time operating above rated torque

ENERGY MANAGEMENT CONTROL PROBLEM

Figure 6 presents a schematic representation of a series hybrid configuration. The power summation node, is an electrical summation node, i.e. power summation is obtained by addition of the electric power from generator and the electric storage.

The basic challenge of energy management in a hybrid electric vehicle is to assure optimal use and regeneration of the total energy in the vehicle. At any time and for any vehicle speed, the control strategy has to determine the power distribution between primary energy converter (FC) and renewable electrical storage system (RESS), as well as the optimal gear ratio of the transmission, if any. These decisions are constrained by two factors. First of all, the motive power

requested by the driver must always be satisfied up to a known limit (maximum power demand).

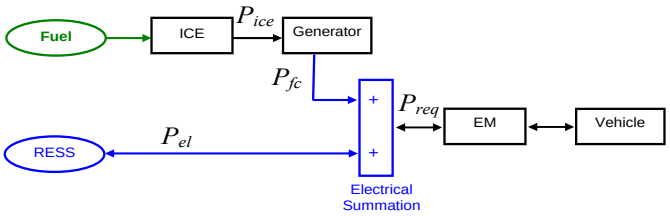

Fig. 6. Power flow representation of a series hybrid configuration.

Secondly, the state of charge of the RESS must be maintained within preferred limits, allowing the vehicle to be charge sustaining. Within these constraints, the first objective is to operate the powertrain in order to achieve the maximum fuel economy. Ideally the motive power must be split at each time to minimize the overall fuel consumption over a given trip, such as:

$$\min_{\{P_{el}(t),P_{fc}(t)\}} \int_0^T \dot{m}_f(\tau)\, d\tau \qquad (1)$$

$$P_{req}(t) = P_{fc}(t) + P_{el}(t) \quad \forall t$$

$$0 < SOE_{\min} \le SOE \le SOE_{\max} \le 1$$

$$0 \le P_{fc}(t) \le P_{fc_{\max}}$$

$$P_{el_{\min}} \le P_{el}(t) \le P_{el_{\max}}$$

where T is the duration of the trip, $\dot{m}_f(t)$ is the fuel flow rate at time t, $P_{el}(t)$ is the power provided by the electrical accumulator at time t, $P_{fc}(t)$ is the power provided by the fuel converter (engine only or engine plus generator depending on the configuration) at time t, and SOE is the state of energy of the RESS and it is related to the energy or charge accumulated in the RESS.

The main problem with this approach is that in order to solve such an optimization problem the whole driving schedule has to be known a priori, thus real-time control cannot be readily implemented. To avoid this drawback, one can replace the global criterion by a local one, reducing the problem to a minimization of the equivalent fuel consumption at each time. The local criteria becomes at all times:

$$\min_{\{P_{el}(t),P_{fc}(t)\}} \dot{m}_{f,eq}(t) \quad \forall\, t \qquad (2)$$

where $\dot{m}_{f,eq}(t)$ is the equivalent fuel flow rate at time t, as defined in the following sections. Note that in a charge-sustaining hybrid any present discharge or charge of the battery must ultimately be balanced by a corresponding future charge or discharge (respectively). This future charge or discharge will result in the fuel converter producing more or less power, thereby consuming more or less fuel than needed to meet the desired power. Thus, some equivalent (future) fuel use can be equated with the present use of the batteries. The equivalent fuel cost $\dot{m}_{f,eq}(t)$ is the sum of the actual fuel consumption rate of the fuel converter, $\dot{m}_{fc}(t)$, and the equivalent fuel use of the RESS, $\dot{m}_{f,RESS,eq}(t)$. The global minimization problem represented in Eq. (1) and the local minimization shown in Eq. (2) are not strictly equivalent. However, local minimization results in a formulation amenable to real-time control, while the use of the equivalent fuel flow rate indirectly accounts for the non-local nature of the problem.

EQUIVALENT FUEL CONSUMPTION MINIMIZATION STRATEGY

The equivalent fuel consumption minimization strategy is based on the assumption of quasi-static behavior of the system. In general, for a normal vehicle, this behavior is characterized by capturing phenomena that are in the order of 0.5-1 sec, while faster dynamics are neglected. The main idea consists in assigning future fuel savings and costs to the actual use of electric energy, and in particular:

- a present discharge of the RESS corresponds to a future fuel consumption that will be necessary to recharge the RESS
- a present RESS charge corresponds to a future fuel savings because this energy will be available in the future to be used at a lower cost

The strategy is charge sustaining because balances the costs in the future with the savings in the future. A schematic representation of this concept is depicted in Fig. 7 and 8. According to this interpretation, the problem of minimizing the fuel consumption given by Eq. (1) can be reformulated as an instantaneous minimization problem as in Eq. (2), where $\dot{m}_{f,eq}(t)$ contains information regarding actual fuel consumption and future fuel saving/cost. In particular, $\dot{m}_{f,eq}(t)$ can be expressed as

$$\dot{m}_{f,eq}(t) = \dot{m}_{f,ICE}(t) + \dot{m}_{f,RESS,eq}(t) \qquad (3)$$

where $\dot{m}_{ICE}(t)$ is the fuel flow rate at time t, while $\dot{m}_{f,RESS,eq}(t)$ is the equivalent fuel cost/saving associated to the RESS.

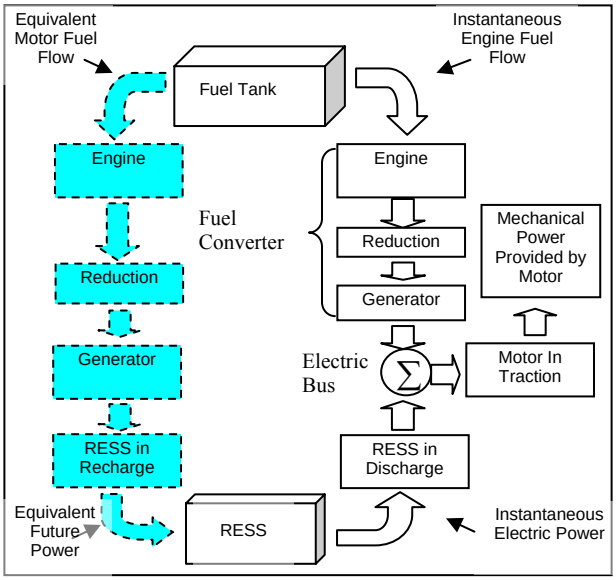

Fig. 7. Energy path for equivalent fuel consumption during RESS discharge.

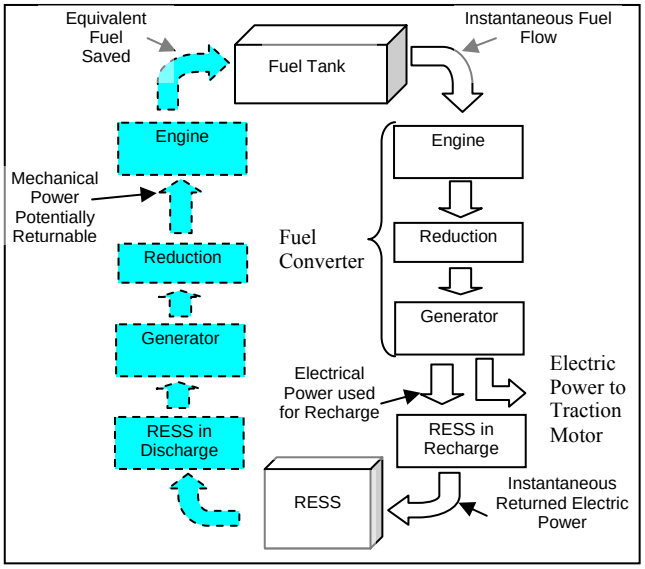

Fig. 8. Energy path for equivalent fuel consumption during RESS recharge

Discharging mode

The amount of energy removed from the RESS at a given power P_{el} during an interval Δt is

$$\Delta E_{RESS,dis} = \Delta t\, P_{RESS,dis} = \frac{\Delta t\; P_{el}}{\eta_{el,dis}(P_{el})} \tag{4}$$

$$\eta_{el,dis}(P_{el}) = \eta_{pe,dis}(P_{el})\,\eta_{RESS,dis}(P_{el}) \tag{5}$$

with $\eta_{pe,dis}$ efficiency of the power electronics that connects the electric storage to the electric bus during discharging, and $\eta_{,RESS,dis}$ efficiency of the electric storage at discharging. The future cost of $\Delta E_{RESS,dis}$

$$c_{\Delta E,dis} = C_{tot,chg}\,\frac{\Delta E_{RESS,dis}}{E_{tot,chg}} \quad [g] \tag{6}$$

where $E_{tot,chg}$ is the total energy recharged in the future to the RESS, and $C_{tot,chg}$ is the cost of $E_{tot,chg}$. This cost is a fraction of the cost of the total energy recharged into the RESS.
The total energy recharged in the future is

$$E_{tot,chg} = \int_{\substack{all\ future\\ rechg.\ cond.}} |P_{RESS,chg}(t)|\,dt + \int_{\substack{all\ future\\ recov.\ cond.}} |P_{RESS,chg}(t)|\,dt \tag{7}$$

The cost of the total energy recharged in the future is

$$C_{tot,chg} = \frac{E_{tot,TANK-RESS}}{Q_{LHV}} \quad [g] \tag{8}$$

$$E_{tot,TANK-RESS} = \int_{\substack{all\ future\\ rechg.cond.}} \frac{P_{fc,RESS}(t)}{\eta_{fc}(t)}dt = \int_{\substack{all\ future\\ rechg.cond.}} \frac{|P_{RESS,chg}(t)|}{\eta_{fc}(t)\eta_{el}(t)}dt \tag{9}$$

where $\eta_{el}(t) = \eta_{pe}(t)\,\eta_{RESS}(t)$, $E_{tot,TANK-RESS}$ is the total energy flowing from the tank to the RESS, Q_{LHV} is the low heating value of the fuel, $P_{fc,RESS}$ is the power from the fuel converter to the RESS, and η_{genset} is the combined efficiency of ICE and generator. By substituting Eq. (7)-(9) into Eq. (6), after some manipulations and approximating the efficiencies by their average values, it can be shown that during discharging

$$c_{\Delta E,dis} \approx \frac{1}{\overline{\eta}_{fc,rechg}\overline{\eta}_{el,rechg}} \cdot \frac{1}{1+\overline{R}_{recov/rech}} \cdot \frac{1}{\eta_{el,dis}(P_{el})} \cdot \frac{P_{el}}{Q_{LHV}}\Delta t$$

where $\overline{\eta}_{fc,rechg}$ is the average efficiency of the fuel converter during recharge, $\overline{\eta}_{el,rechg}$ is the average efficiency of the electric path during recharge, and $\overline{R}_{recov/rech}$ is the average value of

$$R_{recov/rech} = \frac{\int_{\substack{all\ future\\ recov.\ cond.}} |P_{RESS,chg}(t)|\,dt}{\int_{\substack{all\ future\\ rechg.\ cond.}} |P_{RESS,chg}(t)|\,dt}$$

The cost in terms of fuel of discharging the RESS, i.e. the equivalent fuel consumption of the RESS in discharging mode, is

$$\dot{m}_{f,RESS,eq} = \frac{c_{\Delta E,dis}}{\Delta t} \approx \frac{1}{\overline{\eta}_{rechg}} \cdot \frac{1}{\eta_{el,dis}(P_{el})} \cdot \frac{P_{el}}{Q_{LHV}} \tag{10}$$

$$\overline{\eta}_{rechg} = \overline{\eta}_{fc,rechg}\overline{\eta}_{el,rechg} \cdot (1+\overline{R}_{recov/rech})$$

$$\overline{\eta}_{x,rechg} = \frac{1}{T_{rechg}} \int_{\substack{all\ future\\ rechg.\ cond.}} \eta_x(t)dt$$

where T_{rechg} is the future time spent in recharge mode.

Charging mode

The amount of energy added to the RESS at a given power P_{el} during an interval Δt is

$$\Delta E_{RESS,chg} = \Delta t\, P_{RESS,chg} = \eta_{el,chg}(P_{el})\,P_{el}\,\Delta t \tag{11}$$

$$\eta_{el,chg}(P_{el}) = \eta_{pe,chg}(P_{el})\,\eta_{RESS,chg}(P_{el}) \tag{12}$$

with $\eta_{pe,chg}$ efficiency of the power electronics that connects the electric storage to the electric bus during charging, and $\eta_{,RESS,chg}$ efficiency of the electric storage during charging. The future saving (negative cost) associated with $\Delta E_{RESS,chg}$ is

$$s_{\Delta E,chg} = S_{tot,dis}\,\frac{\Delta E_{RESS,chg}}{E_{tot,dis}} \quad [g] \tag{13}$$

where $E_{tot,dis}$ is the total energy discharged in the future, $S_{tot,dis}$ is the saving due $E_{tot,dis}$. This saving is a fraction of the savings due to the total energy discharged from the RESS. The total energy discharged in the future is

$$E_{tot,dis} = \int_{\substack{all\ future\\ dis.\ cond.}} P_{RESS,dis}(t)\,dt \tag{14}$$

The savings due to the total energy discharged in the future is

$$S_{tot,dis} = \frac{E_{tot,RESS-TANK}}{Q_{LHV}} \quad [g] \tag{15}$$

$$E_{tot,RESS-TANK} = \int_{\substack{all\ future\\ dis.cond.}} \frac{\eta_{el}(t)\, P_{RESS,dis}(t)}{\eta_{fc}(t)} dt \qquad (16)$$

where $E_{tot,RESS-TANK}$ is the total energy flowing from the RESS to the tank (virtual). By substituting Eq. (14)-(16) into Eq. (13), after some manipulations and approximating the efficiencies by their average values,, we have

$$s_{\Delta E,dis} \approx \frac{\overline{\eta}_{el,dis}}{\overline{\eta}_{fc,dis}} \cdot \eta_{el,chg}(P_{el}) \cdot \frac{P_{el}}{Q_{LHV}} \Delta t \qquad (17)$$

where $\overline{\eta}_{fc,rechg}$ is the average efficiency of the fuel converter during recharge, and $\overline{\eta}_{el,rechg}$ is the average efficiency of the electric path during recharge.

The cost in terms of fuel of charging the RESS, i.e. the equivalent fuel consumption of the RESS in charging mode, is

$$\dot{m}_{f,RESS,eq} = \frac{s_{\Delta E,dis}}{\Delta t} \approx \frac{1}{\overline{\eta}_{dis}} \cdot \eta_{el,chg}(P_{el}) \cdot \frac{P_{el}}{Q_{LHV}} \qquad (18)$$

$$\overline{\eta}_{dis} = \frac{\overline{\eta}_{fc,dis}}{\overline{\eta}_{el,dis}}, \overline{\eta}_{x,dis} = \frac{1}{T_{dis}} \int_{\substack{all\ future\\ dis.cond.}} \eta_x(t) dt$$

where T_{dis} is the future time spent in discharge mode.

Remark: The efficiencies $\overline{\eta}_{dis}$ and $\overline{\eta}_{rechg}$ are unknown because they depend on the future. It is possible to show that fuel consumption vs. efficiencies $\overline{\eta}_{dis}$ and $\overline{\eta}_{rechg}$ presents a minimum located in a quite broad flat region which is common to all driving cycles. By selecting these efficiencies in this region, variations in fuel consumption with respect to the optimum are within 5%.

SEEKER-FILTER-VIEWER ARCHITECTURE FOR DESIGN SPACE EXPLORATION

The large-scale design-space exploration can be efficiently done by converting the vehicle simulator into C-code and compiling it into executables. The advantage is that executables run much faster and they can be called by the Seeker software [13,14]. This opens the door to massive design space explorations, with the Seeker coordinating many computers simulating different vehicle configurations in parallel and returning the results.

As illustrated in Fig. 9, the Seeker-Filter-Viewer architecture for design-space exploration has three synergistic components

- **Seeker** - generates design alternatives and evaluates them according to multiple criteria,
- **Filter** - selects from the generated alternatives a Pareto-optimal subset. A decision candidate *A* dominates another candidate *B* if *A* is better or equal to *B* in every criterion and is better than *B* in at least one criterion. Any candidate that is dominated by another candidate is discarded. The survivors comprise the Pareto subset. No member of the Pareto subset dominates any other element in the subset (thus, deciding among alternatives in the Pareto set is always a matter of tradeoffs).
- **Viewer** - enables a decision-maker to perform visual trade-off analyses of the elements of the Pareto set and possibly narrow to a subset for further exploration.

The Seeker can use any number of networked computers to evaluate designs in parallel. Thus, the Seeker makes it possible to consider very large numbers of design alternatives.

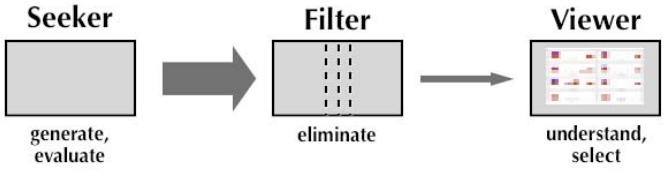

Fig. 9. Seeker-Filter-Viewer architecture.

The ability to explore such large spaces makes it possible for the decision maker to move away from the current dominant practice of exploring variations around a set of known good designs, and towards exploring all regions of a decision space, looking for design nuggets. As illustrated in Fig. 10, the Seeker sits at the center of multiple loops, determining the tunable parameters and receiving the final metrics from another module which calls the simulator and post processor via the appropriate executable calls.

As mentioned, the Filter selects the Pareto-optimal subset from the set of generated designs. In practice, in most domains of application the Filter is able to eliminate most alternatives, most of the time. Moreover as the size of the design space increases, the efficiency in eliminating alternatives increases. This kind of efficiency is extremely important for practical applications of the technology: a decision-maker can have the confidence of having explored large spaces, while needing to study in detail an extremely small percentage of the decision alternatives.

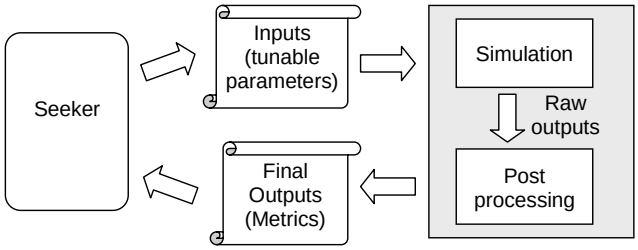

Fig. 10. Seeker-based simulation and evaluation management.

The Viewer is used to interactively explore the surviving design alternatives, and to visualize the trade-offs between pairs of evaluation criteria. The surviving alternatives are presented as a set of scatter plots, one plot for each pair of criteria for which the user wishes to examine the trade-off behavior. The user can select interesting subsets in one plot, perhaps seeing that, in a certain region, for a small decrease in one evaluation criterion, substantial improvement is possible in the other criterion. The user then might select the candidates in that region; perhaps seeing that there are enough candidates with properties in the desirable ends of the scales, so that the ones with less desirable values can be discarded. It is important to note that this kind of decision cannot be made *a priori*; it is the actual distribution of candidates that makes it possible for the

user to make choices. The displays in the Viewer are linked; candidates selected in one plot are simultaneously highlighted in other plots so that a user can immediately see how the selected alternatives fare on other criteria. Subsets may be also selected by structural constraints. The decision maker may narrow to selected regions and study the candidates in greater detail, back out, and then narrow to another region, and so on. Thus, the Viewer is useful for aiding understanding of the design space, as well as enabling narrowing the choice to favorable candidate designs, or down-selecting to a single best design.

The following section demonstrates how the viewer (along with the filter) allows the user to interactively exploring the design space. Figure 11 (along with some later Figs.) presents a screen capture of an interactive session. The user sees the design candidates in multiple tradeoff plots. Candidates are plotted with an "x" and the candidates the user has selected are highlighted in red.

SIMULATION RESULTS

To better illustrate how the design space exploration works, some results for a U.S. Army FMTV (Family of Medium Tactical Vehicles) are reported. The characteristics of the basic conventional vehicle are summarized in Table 2. The main objective was to design a hybrid electric FMTV for improved fuel consumption and better performance. To achieve this result, numerous design configurations were analyzed using the Seeker-Filter-Viewer tool. As a first step in the elimination of the possible candidates, a 60% gradability test was conducted by simulation for all the configurations. As a result, 75 candidates unable to move were discarded from further consideration.

Focusing on the survivors, on- and off-road performance and economy metrics in the various tradeoff windows were analyzed. Figure 12 shows the various plots initially used for the exploration. The Y axis elements correspond to "economy/efficiency" metrics and the X axis elements correspond to performance metrics. The exception here is the fourth plot, in the lower right corner, which shows two performance metrics for off-road conditions. The upper left window shows on-road performance and economy while the lower left window shows off-road performance and economy. Looking at the lower left and lower right plots one can notice that the X axis has been "flipped" (numbers decrease from left to right)—so that "good" values are always to the left. The upper left corner of the upper right plot was selected (Fig. 12), highlighting vehicles with good ability to "recapture" energy and good performance in on-road situations. As the other plots indicate these points (shown in red) show reasonable performance and efficiency across the range of different tests and metrics. As the other plots indicate these points (shown in red) show reasonable performance and efficiency across the range of different tests and metrics.

Next, the configurations that presented poor on-road performance were discarded. Candidates were further filtered to eliminate points with poorer off-road performance and fuel economy. Remaining candidates were examined by comparing the on-road fuel consumption. After deleting the inferior candidates according to this criterion, the weight (mass) impact of the various powertrain components was considered. Figure 13 shows a histogram indicating the additional mass of the powertrain. The candidates that were able to regenerate the largest percentage of available energy (red) and those with the lightest powertrains (purple) were selected. A highlighting color (gold) represents the intersections of these two preferences. Powertrains with large engines and supercapacitors were strongly favored (Fig. 14).

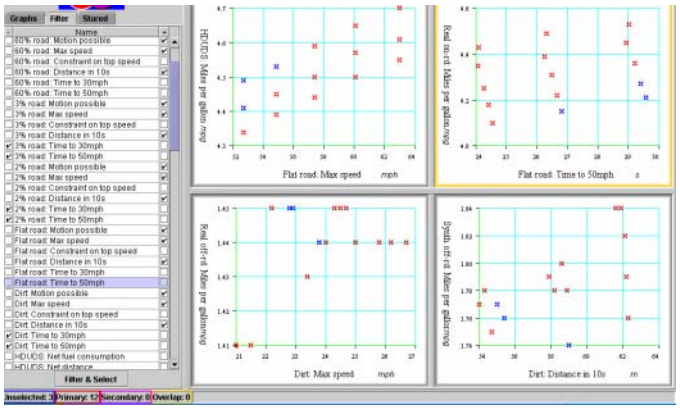

Fig. 11. Different alternatives in the Viewer.

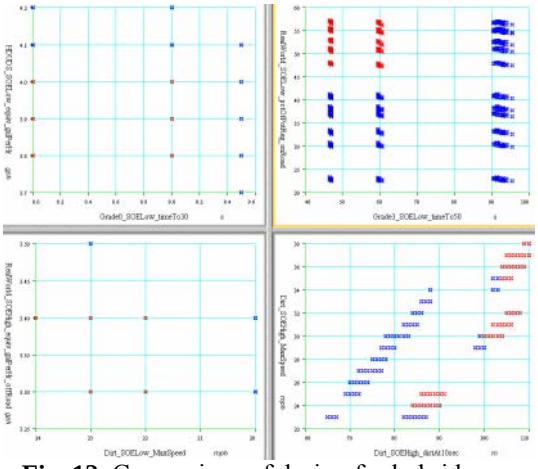

Fig. 12. Comparison of design for hybrid.

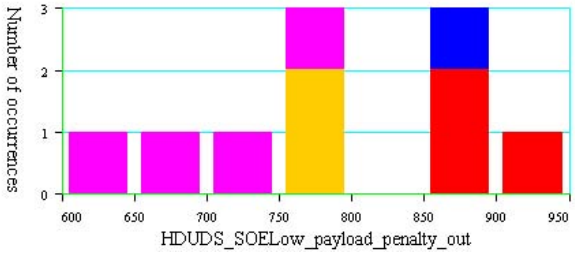

Fig. 13. Further exploration of HEV design space, investigating mass impact of powertrain choices.

After some rethinking, the impact of placing a stronger preference on lighter weight powertrains during the early phases of the design was considered. Using the "redo" functionality provided by the viewer, it was possible to step all the way back to the very first "tradeoff" choice (Fig. 12). The graph in the lower right was then modified to show a histogram of the additional powertrain mass (with respect to the conventional) as depicted in Fig. 15. Here the light powertrain configurations are highlighted in purple, with the vehicles

having "good ability" to recapture energy and good on road performance still highlighted in red (as in Fig. 12). The intersection of these two preference sets (red and purple) are then shown in gold. These "preferred" candidates (under the increased emphasis for reduced mass) are shown in Table 3.

Color	Axle Ratio	ICE HP (hp)	Generator (kW)	Storage Type	Cap # Parallel	Cap # Series	Traction Motor Peak Torque (Nm)	Cap R (ohm)
	10.2	355.0	305.0	1.0	3.0	250.0	748.0	7.0E-4
	10.6	355.0	305.0	1.0	3.0	250.0	748.0	7.0E-4
	9.0	355.0	305.0	1.0	2.0	250.0	941.0	7.0E-4
	9.0	355.0	305.0	1.0	2.0	250.0	844.0	7.0E-4
	10.6	355.0	305.0	1.0	2.0	250.0	748.0	7.0E-4
	10.6	355.0	305.0	1.0	3.0	250.0	748.0	0.0010
	9.0	355.0	305.0	1.0	3.0	250.0	941.0	7.0E-4
	9.0	355.0	305.0	1.0	3.0	250.0	844.0	7.0E-4
	10.6	355.0	305.0	1.0	3.0	250.0	844.0	7.0E-4
	9.0	355.0	305.0	1.0	3.0	250.0	844.0	0.0010

Fig. 14. Highlighted options (storage type: 1-caps, 2-batteries).

Table 3. Preferred design alternatives (when powertrain mass becomes a primary decision factor)

Final drive ratio	ICE power [hp]	Generator power [kW]	Storage type	Cap # parallel	Cap # series	Cap R [ohm]	Traction motor peak torque [Nm]
9.8	330	285	caps	1	250	7e-4	748
9.8	330	285	caps	1	250	1e-3	748
10.2	330	285	caps	1	250	7e-4	748
10.2	330	285	caps	1	250	1e-3	748
10.6	330	285	caps	1	250	7e-4	748
10.6	330	285	caps	1	250	1e-3	748

ACKNOWLEDGMENTS

This work was sponsored by the US Army Tank-automotive and Armaments Command (TACOM), under contact # DAAE07-03-C-L134. The views and conclusions contained in this document are those of the authors and should not be interpreted as representing the official policies, either expressed or implied, of the U. S. Army or the U. S. Government.

REFERENCES

[1] Gillespie, T. *Fundamental of Vehicle Dynamics*, Society of Automotive Engineers, Inc., 1992.

[2] Zou, Z., Davis, S., Beaty, K., O'Keefe, M., Hendricks, T., Rehn, R., Weissner, S., Sharma, V., "A New Composite Drive Cycle for Heavy-Duty Hybrid Electric Class 4-6 Vehicles," SAE paper 2004-01-1052, March 2004.

[3] Bekker, M. G. *Theory of Land Locomotion: The Mechanics of Vehicle Mobility*. 1956. University of Michigan Press, Ann Arbor, MI.

[4] Bekker, M. G. *Off-the-Road Locomotion: Research and Development in Terramechanics.* 1960. University of Michigan Press, Ann Arbor, MI.

[5] Bekker, M. G. *Introduction to Terrain-Vehicle Systems*. 1969. University of Michigan Press, Ann Arbor, MI.

[6] Chandrasekaran, A.K., *Vehicle Design Optimization Using Multibody Dynamic Simulation and Large Design Space Search Methods*, Masters Thesis, The Ohio State University, 2002.

[7] Rizzoni, G., Guzzella, L., and Baumann, B. M., "Unified Modeling of Hybrid Electric Vehicle Drivetrains", *IEEE/ASME Trans. on Mechatronics*, vol. 4, no. 3, pp. 246–257, 1999.

[8] Lin, C. C., Kang, J. M., Grizzle, J. W., and Peng, H., "Energy Management Strategy for Parallel Hybrid Electric Truck", in *Proc. American Control Conference*,VA, June 2001, pp. 2878–2883.

[9] Sciarretta, A., Guzzella, L., Onder, C. H., "On the Power Split Control of Parallel Hybrid Vehicles: from Global Optimization towards Real-time Control", in *Automatisierungstechnik 51 (2003) 5.*

[10] Paganelli, G., Ercole, G., Brahma, A., Guezennec, Y. and Rizzoni, G., "General Supervisory Control Policy for the Energy Optimization of Charge-Sustaining Hybrid Electric Vehicles" in *JSAE Review* 22 (2001), pp 511-518.

[11] Paganelli, G., Tateno, M., Brahma, A., Rizzoni, G. and Guezennec, Y., "Control Development for a Hybrid-Electric Sport-Utility Vehicle: Strategy, Implementation and Field Test Results", in *Proc. American Control Conference*, VA, June 2001, pp. 5064–5069.

[12] Pisu, P., Musardo, C., Staccia, B., and Rizzoni, G., "A Comparative Study of Supervisory Control Strategies for Hybrid Electric Vehicles". *IMECE 2004*, 13-19 November 2004, Anaheim, CA.

[13] *Visualization Environment* developed by Aetion Technologies LLC (http://www.aetion.com) in collaboration with the Ohio State University (http://www.osu.edu).

[14] Josephson, J.R., Chandrasekaran, B., Carroll, M., Iyer, N., Wasacz, B., Rizzoni, G., Li, O., Erb, D. A., *An Architecture for Exploring Large Design Spaces*, National Conference on AI (AAAI-98), American Association for Artificial Intelligence, 1998.

[15] Heywood, J.B., *Internal Combustion Engine Fundamentals*, 1988, McGraw Hill, New York.

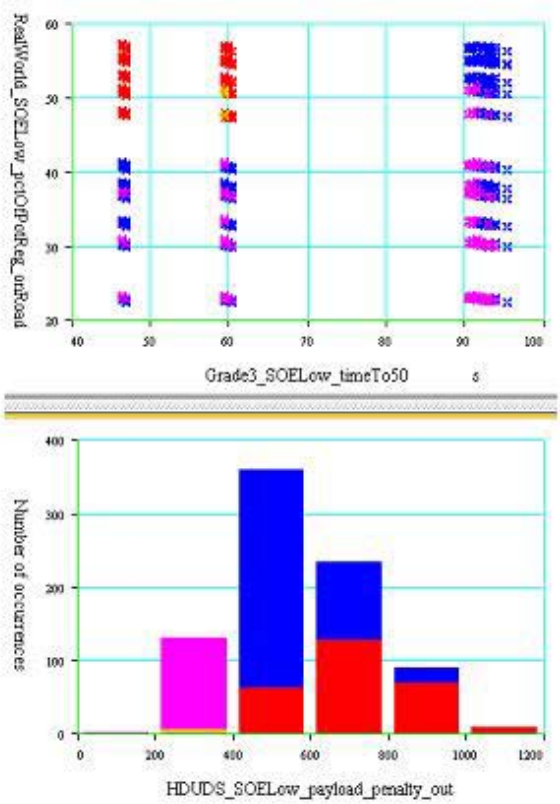

Fig. 15. Reconsidering the downselection by giving earlier attention to the powertrain mass.